

The shock-waves interference in the flow around a cylinder mounted on a blunted plate

Volf Borovoy, Vladimir Mosharov, Vladimir Radchenko, and Arkady Skuratov
Central Aerohydrodynamic Institute (TsAGI), Zhukovsky, Moscow Region, Russia

Abstract

The hypersonic flow around a cylinder mounted on sharp and blunted plates was investigated experimentally. Experiments were conducted in shock wind tunnel at Mach $M=5$ in wide range of Reynolds numbers $Re_{\infty L}$ (calculated by plate length) from 0.8×10^7 to 3.4×10^7 . Cylinder distance from plate leading edge X_0 and plate bluntness radius r was varied. Optical Temperature Sensitive Paint (TSP) method was used for heat transfer investigation, as well as other optical method of surface flow visualization. The results of investigations of flow structure and heat transfer in the interference zone on the plate surface ahead of cylinder and in his vicinity are presented. It is shown that laminar-turbulent boundary layer transition on the plate and his reverse leads to non-monotonic dependences of heat flux peak values in interference zones on X_0 and r values.

1. Introduction

The problem of flow around a cylinder mounted on a plate draw attention of scientific society in the sixties of the last century [1-11]. Flow around a cylinder installed on sharp plate at large distance from plate leading edge was studied. Main features of flow structure were investigated and sharp peaks of heat flux and pressure were discovered on the plate ahead of cylinder and on the cylinder. Investigations show that flow three-dimensionality ahead of cylinder leads to significant increase of heat flux and pressure peak values in respect with two-dimensional case.

The development of supersonic vehicles inlets draws an additional attention to the problem of flow around cylindrical obstacle since inlet compressing wedge and cowl edges should be blunted to restrict their temperature. Also the inlet of a rectangular cross-section is usually restricted by sidewalls to prevent compressed air losses, and leading edges of these sidewalls should be blunted also. The distance from sidewalls leading edges to compressing wedge and cowl edges can be rather small, that restricts the size of separation zone ahead of cylinder and can cause significant change of heat flux and pressure distributions in respect with the case of free boundary layer separation at large distance from plate leading edge. That is the problem of interaction of cylindrical shock waves generated by blunted plate and cylindrical obstacle at different distances from plate leading edge exists.

In present work the distance from plate leading edge to the cylinder was varied in wide range. In these conditions the boundary layer ahead of cylinder is in the laminar, transient or turbulent state depending on distance and on plate leading edge bluntness. Both the free interaction of bow cylinder shock wave with plate boundary layer, as well as the flow with fixed separation line position (on the plate leading edge) was realized. Flow structure was investigated on sharp and blunted plates. It was shown that plate blunting affects significantly the flow and heat flux near the cylinder. This influence is especially significant at small distances from plate leading edge to the cylinder.

2. Model, Experimental conditions, Investigation methods

Model schematic is shown on Figure 1. On the flat plate 1 with variable leading edge bluntness r (by changing insert 3) the vertical plate 2 having cylindrical leading edge of radius $R=5$ mm is installed. Distance from flat plate leading edge to vertical plate cylindrical leading edge X_0 can be varied in wide range. Some experiments were also made without vertical plate to determine the state of undisturbed boundary layer on flat plate. For heat flux investigation the flat plate insert 5 was made of thermo-insulating material – fiberglass AG-4. For schlieren visualization the other insert with rectangular optical glass window was used.

Experiments were made in shock tube UT-1M of TsAGI, operated in Ludwig mode, at Mach number $M=5$ and at two total temperatures: $T_0 \approx 610$ K ($T_w/T_0=0.48$) in the experiments without vertical plate and $T_0 \approx 450$ K ($T_w/T_0=0.64$) in the experiments with vertical plate to decrease model surface overheating in the regions of peak heat fluxes. Reynolds number $Re_{\infty L}$ calculated by flat plate length $L=377$ mm and free stream parameters was varied in the range from 0.8×10^7 to 3.4×10^7 by changing the total pressure (from 16 to 65 bar) and total temperature (450 and 610 K). The duration of the flow with stable parameters is 40 ms (total duration is 120-130 ms). Nozzle outlet diameter is 300 mm.

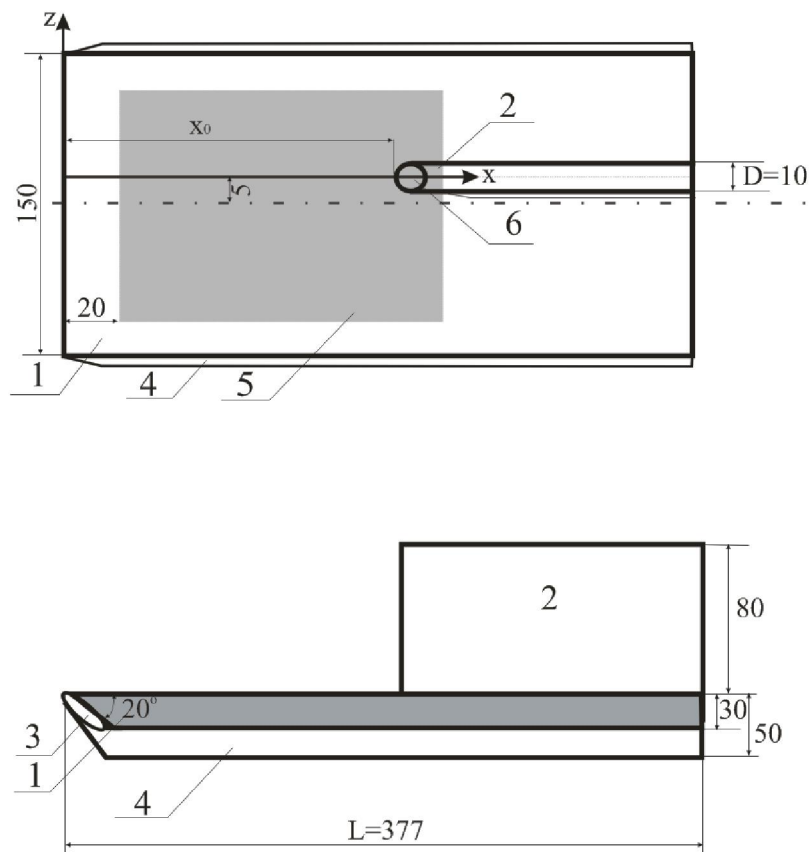


Figure 1: Model schematic: 1 – flat plate, 2 – vertical plate with cylindrical leading edge, 3 – changeable plate leading edge insert, 4 – side fences, 5 – flat plate insert, 6 – cylinder.

Heat flux coefficient was measured with Temperature Sensitive Paint (TSP) – thin luminescent paint, sensitive to the temperature [12]. To realize heat flux measurements, the investigated surfaces were made of material having low thermoconductivity – fiberglass AG-4. Surface streamline visualization on flat plate and on the cylinder was realized with Particle Image Surface Flow Visualization (PISFV) method [13] based on application viscous oil containing luminescent particles.

3. Flow structure, Separation zone configurations

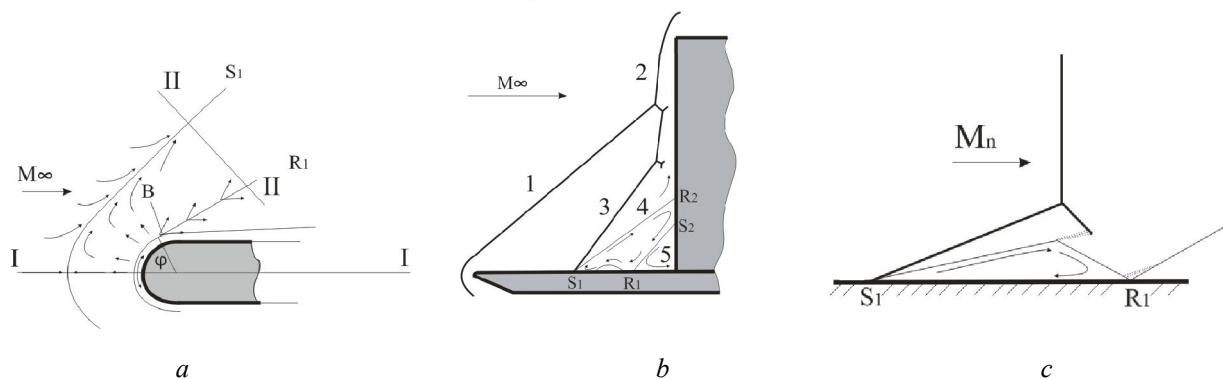


Figure 2: Flow structures: *a* – surface streamlines on flat plate, *b* – I-I section, *c* – II-II section; 1, 2 – bow shock waves of flat and vertical plates, 3 – separation shock, 4 – global separation zone boundary, 5 – local separation zone; S_1 , S_2 – convergence lines, R_1 , R_2 – divergence lines.

Flow structure for the case of blunted flat plate is shown on Figure 2. Primary separation line S_1 and reattachment line R_1 caused by the global separation ahead of cylinder are formed on the flat plate. Reattachment line (R_2) is formed on the vertical cylinder, and gas flows from this line along vertical cylinder surface to the flat plate, separates

secondarily on line S_2 and reattaches to the plate on line R_1 . At some conditions the secondary separation zone becomes very small and reattachment line R_1 is located on flat plate in nearest vicinity to vertical cylinder.

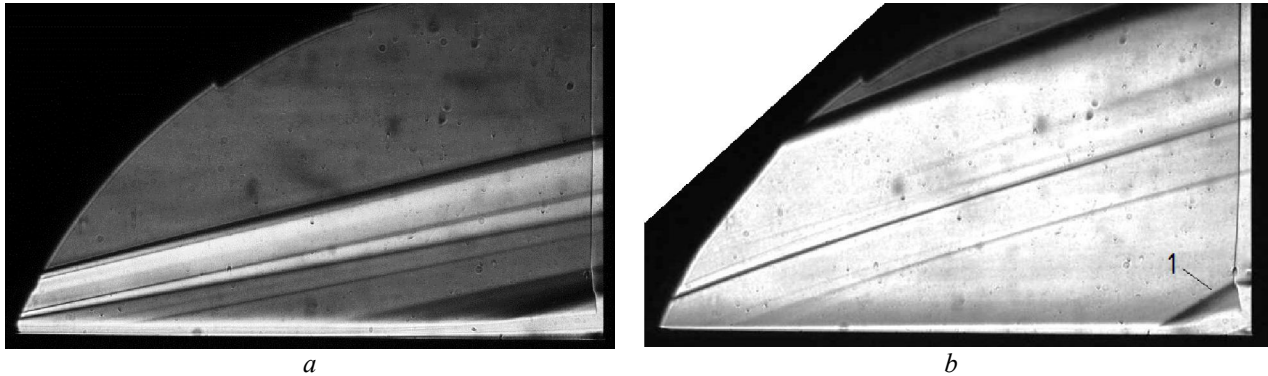


Figure 3: Schlieren photos at $X_0/D=15$: $a - r=0$, $Re_{\infty L}=1.1 \times 10^7$, laminar separation, $b - r=4$ mm ($r/X_0=0.027$), $Re_{\infty L}=1.9 \times 10^7$, turbulent separation; 1 – separation shock.

Figure 3 shows typical schlieren photos of laminar and turbulent separation zones formed ahead of cylindrical vertical plate. It is well known that laminar separation zone is longer and inclination angle of its boundary is smaller than that of turbulent separation. A set of these schlieren photos allows to get the dependences of separation zone length l_s and of its boundary inclination angle θ_s on the distance of vertical plate from flat plate leading edge X_0 and on flat plate bluntness radius r .

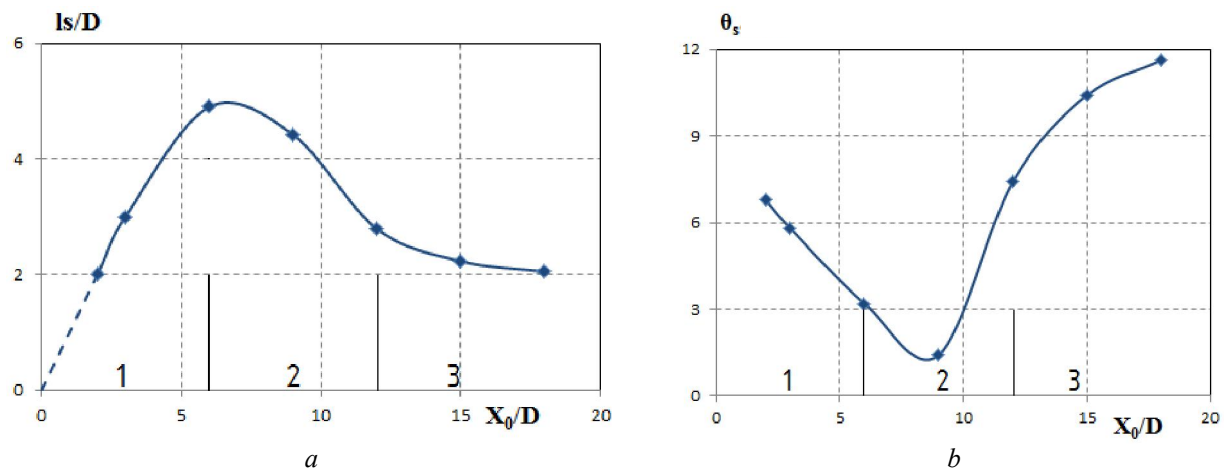


Figure 4: An influence of the distance from flat plate leading edge to the cylinder on separation zone parameters at $r=0$ and $Re_{\infty L}=1.9 \times 10^7$: a – separation zone length, b – inclination angle of separation zone boundary; 1 – laminar boundary layer, 2 – transient boundary layer, 3 – turbulent boundary layer ahead of separation line.

Separation zone parameters are changing non-monotonically with an increase of distance from flat plate leading edge to vertical cylinder (Fig.4). This non-monotony is caused by laminar-turbulent transition of boundary layer on flat plate (boundary layer state ahead of separation line was determined from heat flux coefficient measurements). At the laminar state of boundary layer, the separation zone becomes longer with an increase of X_0 because of boundary layer thickening. Inclination angle of separation zone boundary is increasing simultaneously. This data corresponds well to the previous results [14], where $l_s/D \sim Re_x^{1/4}$ and $\theta_s/D \sim Re_x^{-1/4}$. Later the separation zone becomes shorter because of laminar-turbulent boundary layer transition.

Flat plate blunting also changes separation zone parameters (Fig.5) because of generation of high-entropy layer after the bow shock wave. This high-entropy layer affects the separation zone by two ways: 1) it increases the total thickness of low-impulse wall layer (boundary layer + high-entropy layers), and 2) it changes the position of boundary layer transition. Figure 5 shows that an increase of flat plate bluntness radius r at the stable position of cylinder ($X_0=150$ mm) changes the length of separation zone non-monotonously. Boundary layer on sharp plate ahead of cylinder is in the turbulent (or practically turbulent) state. Small plate leading edge blunting (up to $r/X_0 \approx 0.05$) leads to the shift of boundary layer transition down the stream, that means that boundary layer ahead of cylinder becomes more laminar, as a result the length of separation zone is increased, but angle θ_s – is decreased. Then the reverse of boundary layer transition takes place and boundary layer is transformed back into turbulent state

ahead of cylinder, that leads to inverse behaviour of l_s and θ_s values. The changes of the separation zone shape and size caused by the reverse of boundary layer transition is also clearly visible on Figure 3: turbulent separation zone on blunted plate ($r=4$ mm) is significantly shorter and its angle θ_s is significantly larger than the laminar one on the sharp plate.

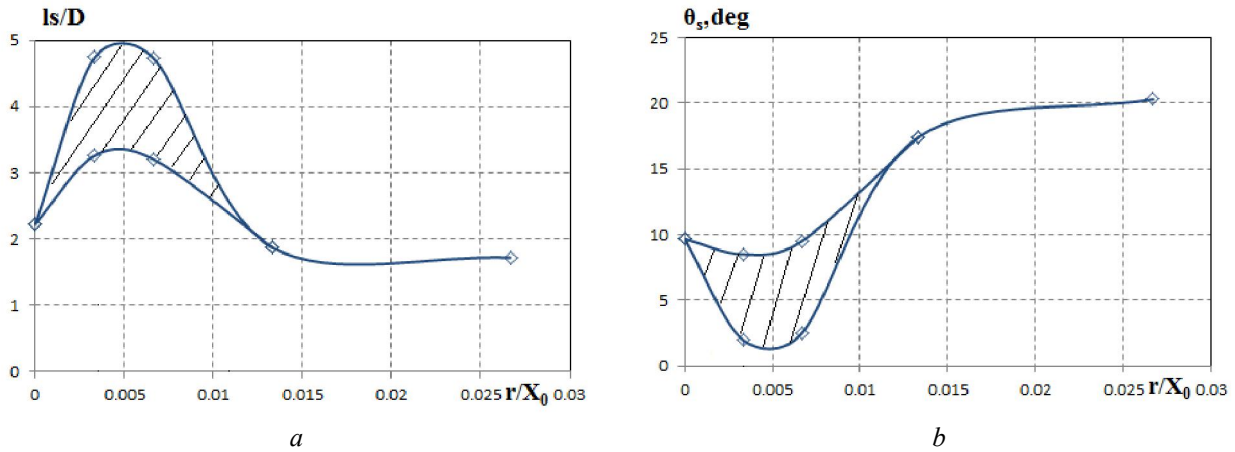


Figure 5: An influence of flat plate bluntness on separation zone parameters at $X_0=150$ mm ($X_0/D=15$) and $Re_{\infty L}=1.9 \times 10^7$: a – separation zone length, b – inclination angle of separation zone boundary.

In some range of bluntness radius ($r/X_0=0.025-0.075$), two configurations of separation zone, corresponded to laminar and turbulent state of boundary layer ahead of separation zone, were observed on schlieren photos simultaneously. May be they were interchanged with high frequency (dozens of kilohertz) that may be caused by instability of boundary layer transition position in this range of bluntness radius. This range is marked by hatching on figure 5.

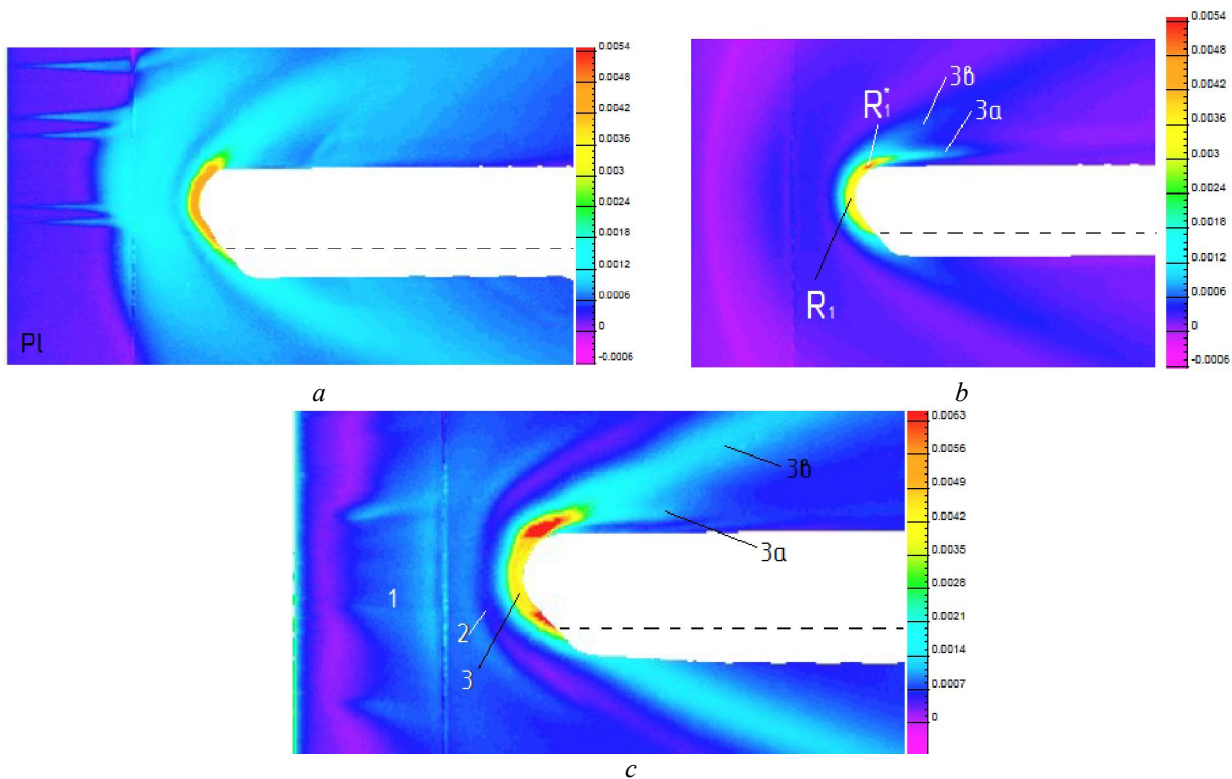


Figure 6: Stanton-number distribution on flat plate surface: $a - Re_{\infty L}=3.16 \times 10^7$, $r=1.0$ mm; $b - Re_{\infty L}=0.92 \times 10^7$, $r=1.0$ mm; $c - Re_{\infty L}=3.2 \times 10^7$, $r=0$ mm. R_1 and R_1^* – heat flux peaks on flat plate.

4. Features of heat transfer distribution on the plate surface

In the vicinity of all the divergence lines shown in Figure 2, there is a local increase in heat transfer. Figure 6 shows typical distributions of the Stanton number on the plate surface near the cylindrical obstacle. In region 1 (Fig.6,c), located behind the global separation line, the heat flux is amplified due to the pressure increase behind the separation shock. Further, there is a narrow region of reduced heat transfer (region 2). It appears due to the formation of the local separation zone (zone 6 in Figure 2) inside the global separation zone. The heat flux coefficient reaches a maximum at the end of the global separation zone (in region 3, Figure 6,c). This semicircle region bifurcates near the lateral generatrix of the cylinder: one branch (3a) extends along the lateral surface of the vertical plate, and the other branch (3b) continues along the bow shock wave of the cylinder.

Figure 6 shows three variants of the heat transfer distribution near the cylinder, differing in the location of the heat flux peak: 1) Figure 6,a – the Stanton number reaches maximal value at the front cylinder generatrix; the Stanton number distribution is symmetric; 2) Figure 6,b – the Stanton number reaches a maximum at one of the lateral generatrices of the cylinder, the St-distribution is asymmetric; 3) Figure 6,c – the Stanton number reaches the peak values at both lateral generatrices of the cylinder, the St-distribution is close to the symmetric one. There is not established a strict regularity of the forming of one or another variant of heat transfer distribution. However, it is noted that at small distances of the vertical plate ($X_0/D=3$), the lateral peaks are formed in all investigated range of Reynolds numbers if the relative bluntness radius of the plate is $r/X_0 < 0.05$. At large distance of the vertical plate from the leading edge (at $X_0/D \geq 15$) and $Re_{\infty L} = 1 \times 10^7$, the lateral peaks are formed only on sharp plate, and at $Re_{\infty L} \geq 1.4 \times 10^7$ – also on the blunted plate ($r=1$ mm). Thus, an increase of Reynolds number or sharpening of the plate promotes the formation of lateral peaks. The formation of one or two side peaks is random.

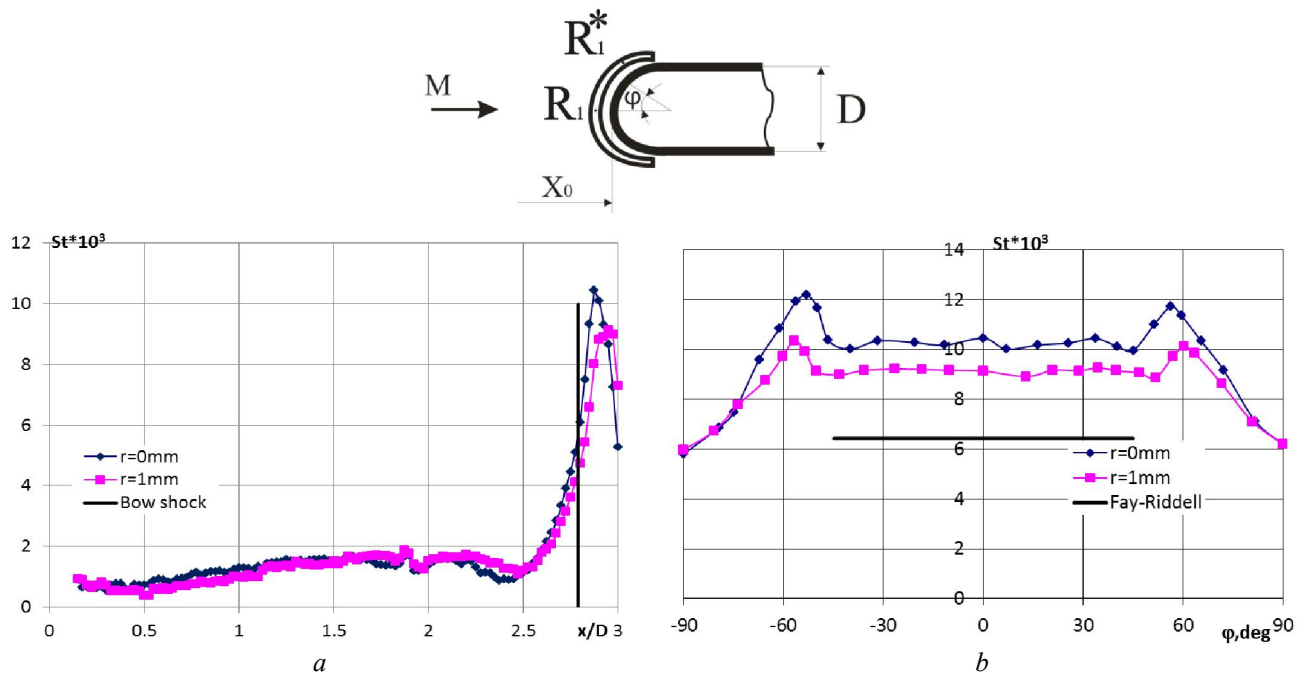


Figure 7: St-distribution on the plate surface at $Re_{\infty L} = 1.4 \times 10^7$ and cylinder distance $X_0 = 30$ mm ($X_0/D = 3$): a – along the symmetry line, b – in the transverse direction (along the line $R_1 - R_1^*$) (Fay-Riddell value – for the front line of the cylinder in undisturbed flow).

Figures 7 and 8 give quantitative information on heat transfer for different values of Reynolds number. In the first example ($Re_{\infty L} = 1.4 \times 10^7$, Figure 7), the Stanton number is increased 10-11 times in front of the cylinder on the symmetry line, and additionally by 20% near one of the lateral generatrices of the cylinder ($\varphi \approx 70$ degrees). In the second example at much larger Reynolds number ($Re_{\infty L} = 3.2 \times 10^7$, Figure 8), the heat transfer on the symmetry axis is increased approximately 11 times, and additionally by 20-30% near the lateral generatrices of the cylinder. Below we consider the possible causes of additional heat transfer near the lateral generatrices of the cylinder.

Analysis of the surface streamlines patterns, obtained earlier in long-duration wind tunnel [8, 14] and in the course of this study, indicates that a specific point is formed on the surface of the horizontal plate near the cylindrical obstacle (point B in Figure 2,a). It is located on a ray inclined on 60-80 degrees to undisturbed flow direction. In the region located between the symmetry line and the point B ($\varphi_B > \varphi > 0$), the stream, separated from the plate surface (on the line S_1 , Figure 2), attaches to the front obstacle surface first (on the line R_2), then separates secondarily (on the line S_2), and only then attaches to the surface of the horizontal plate (on the divergence line R_1). In the region located beyond

the point B , the flow, separated on the line S_l , after the turn attaches directly to the surface of the horizontal plate on the line R_l . From the point B , the surface streamlines emerge in two directions: along the lateral surface of the vertical plate and at an angle to this surface. Accordingly, the vortices formed ahead of cylinder bifurcates beyond the point B : one branch extends along the flat surface of the vertical plate, and the other one along the bow shock wave of the cylinder. Because of three-dimensional character of the flow, the pressure gradient in the vicinity of the point B can be much larger than that in the other points of the divergence line. This may be one of the reasons for the local enhancement of heat transfer near the point B .

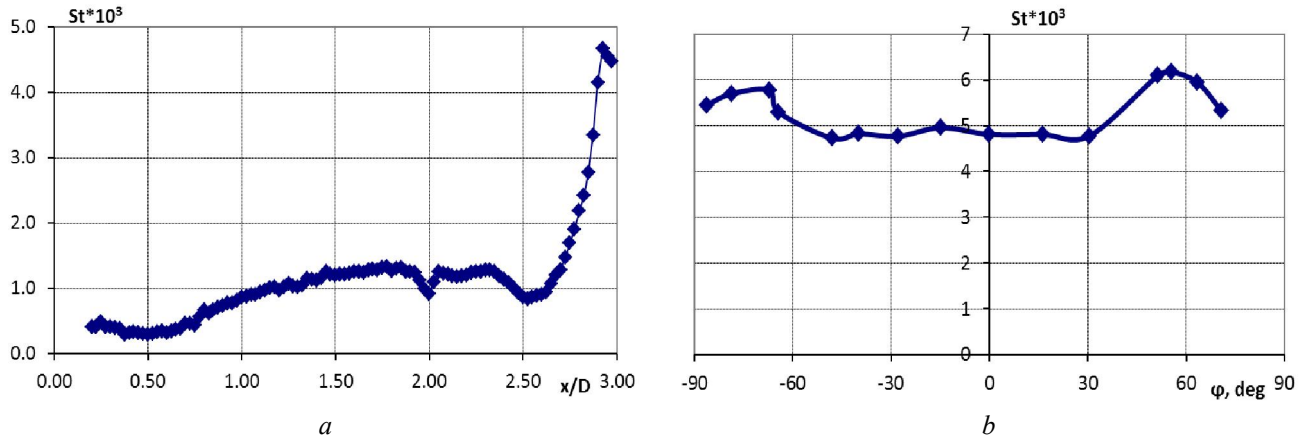


Figure 8: Stanton-number distribution on flat plate surface at $Re_{\infty L} = 3.5 \times 10^7$, cylinder distance $X_0 = 30$ mm and $r = 0$: a – along the symmetry line, b – in the transverse direction (along the line $R1-R1^*$).

A more probable reason of heat transfer enhancement in the vicinity of the point B is associated with the laminar-turbulent transition within the global separation zone. In spite of the turbulence of undisturbed flow, the laminar boundary layer is formed near the divergence point R_1 . However, then, at some distance from the point R_1 , the laminar boundary layer can transform to the turbulent state. This can be facilitated by disturbances presented in the incoming turbulent boundary layer, or generated by irregularities on the horizontal plate. This assumption is supported by irregular formation of zones of enhanced heat transfer near the side generatrices of the cylinder: in some regimes under approximately identical conditions, additional heating occurs on either side of the symmetry line, or on one side of this line, or does not occur at all.

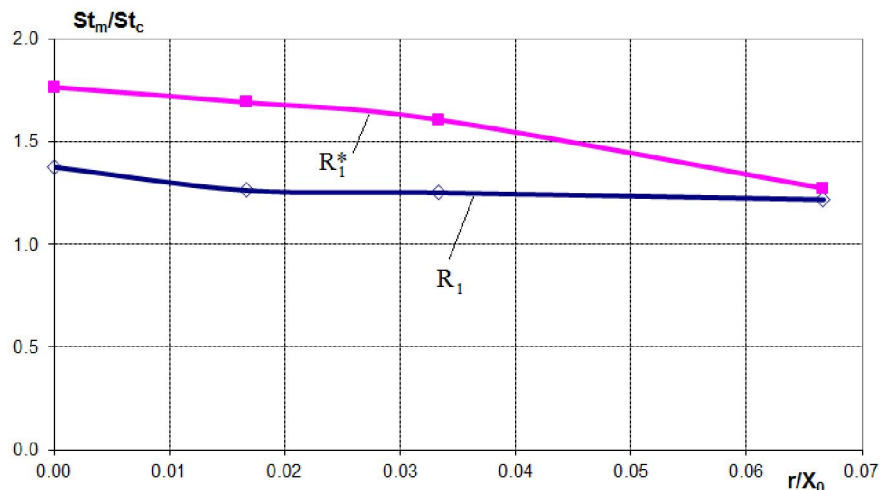


Figure 9: Stanton-number peak values vs plate bluntness radius at $Re_{\infty L} = 3.4 \times 10^7$ and $X_0 = 30$ mm.

5. Influence of the plate bluntness and the cylinder distancing on the peak St -values on the horizontal plate

Figure 9 shows the dependence of maximal St -value on the plate leading edge bluntness radius, and Figures 10, a, b – its dependence on distance between the vertical plate and the leading edge of the horizontal plate. The maximum heat flux values on the plate near the cylindrical obstacle exceed many times the heat flux values in undisturbed region and are of the order of heat flux magnitude on front cylindrical surface of vertical plate. Therefore, in Figures 9 and

10, the peak Stanton number values St_m are related to the Stanton value St_c calculated by Fay-Riddell formula for the cylinder of $D=10$ mm diameter in undisturbed flow.

Figure 9 shows that Stanton-number maximum near the cylindrical obstacle decreases with an increase of flat plate bluntness. This effect is caused by the thickening of low-impact layer (boundary layer + high-entropy layer), that leads to the decrease of velocity gradient on the diverging line.

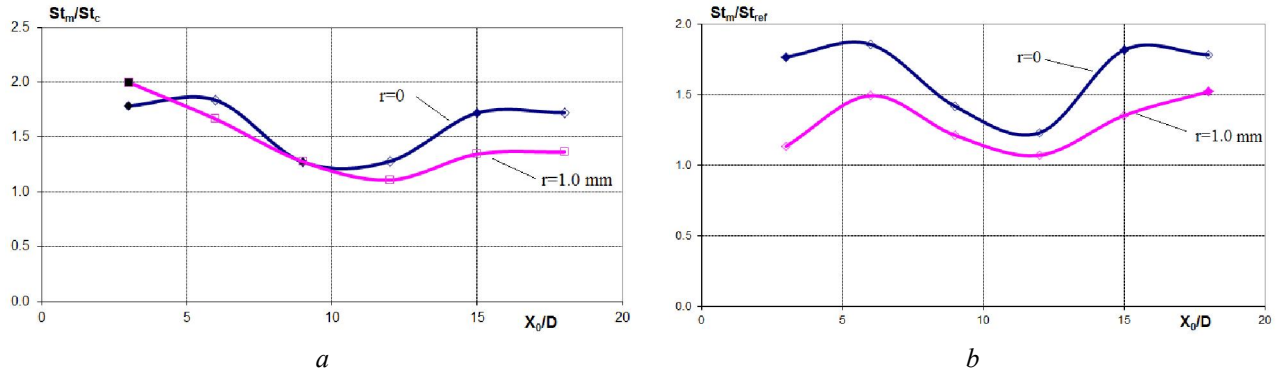


Figure 10: Stanton-number peak values vs the distance from the plate leading edge to cylindrical obstacle (the light markers correspond to the location of the peak near the symmetry line, the dark markers correspond to the far distance of the peak from the symmetry line): $a - Re_{\infty L} = 1.0 \times 10^7$, $b - Re_{\infty L} = 3.4 \times 10^7$.

At the increase of the distance between the vertical plate and the leading edge of the horizontal plate, the peak values of the Stanton number change non-monotonically (Figures 10,a,b). This dependence agrees with nonmonotonic change in the length of the separation zone, formed ahead of cylindrical obstacle, and in the inclination angle of the separation-zone boundary (Figure 4). However, in all investigated cases the peak value of the Stanton number on the plate exceeds the Stanton-number value, calculated for the divergence line on the cylinder in undisturbed flow.

The dependence of St -number peak values on the obstacle distancing (Figure 10) reveals an interesting feature: at smaller Reynolds number (Figure 10,a), there is no clear tendency to reduce the ratio St_m/St_c as X_0/D approaches zero, in spite of degeneration of separation zone (Figure 4,a). An attempt to make additional measurements of heat transfer coefficient were made for small values of X_0/D (0.5, 1 and 2; $Re_{\infty L} = 1.4 \times 10^7$). Unfortunately, quantitative data can not be obtained since main plate has not insulating insert near the leading edge and thermal properties of steel edge coated by thin organic paint can not be determined precisely to calculate heat flux values from TSP measurements. However, the qualitative results of these experiments indicate that the maximum heat transfer coefficient continues to increase at approaching of the cylinder to the plate leading edge. Apparently, this is caused by the thinning of boundary layer, similarly to the case of non-separated flow.

Conclusion

An experimental study of the flow structure and heat transfer on a plate near a cylindrical obstacle at Mach number $M=5$ and Reynolds numbers $Re_{\infty L}$ from 0.8×10^7 to 3.4×10^7 under laminar, transient and turbulent states of undisturbed boundary layer is carried out. An influence of plate bluntness-radius and the distance of the obstacle from plate leading edge on the gas flow is studied.

It is shown that the length of the separation zone, formed on the plate in front of the cylinder, and the inclination angle of its boundary are varying depending on the cylinder distancing from the plate leading edge and on the plate bluntness radius non-monotonically. This effect is caused by laminar-turbulent transition of plate boundary layer and by the reversal of boundary layer transition.

The formation of a narrow semi-annular zone of enhanced heat flux on the plate in front of the cylinder in the vicinity of the divergence line was confirmed. It is shown that heat-transfer coefficient in this zone is many times higher than that in undisturbed region; moreover, it is also greater than heat-transfer coefficient calculated for the front surface of the cylinder in undisturbed flow.

In some experiments an anomalous distribution of heat-transfer coefficient on the plate near the cylinder was observed: the heat-transfer coefficient reaches a maximum value not at the front generatrix of the cylinder, but at its lateral generatrices. The peak value of the heat-transfer coefficient at the lateral generatrices can be 50-60% larger than at the front generatrix. These data need additional verification and explanation.

The work was supported by the Russian Foundation for Basic Research (projects 14-01-00378 and 17-01-00339).

References

- [1] Voitenko D.M., Zubkov A.I., Panov Yu.A. 1966. Flow past a cylindrical obstacle on the plate by a supersonic gas flow. In: *Izvestiya of the USSR Academy of Sciences, MZHG, No. 1.* 121-125 (in Russian).
- [2] Avduevsky V.S., Medvedev K.I. 1967. Physical features of the flow in the separation region with the three-dimensional interaction of the boundary layer with the shock wave. In: *Izvestiya of the USSR Academy of Sciences, MZHG, No. 1.* 25-33 (in Russian).
- [3] Voitenko D.M., Zubkov A.I., Panov Yu.A. 1967. On the existence of supersonic zones in three-dimensional detachment flows. In: *Izvestiya of the USSR Academy of Sciences, MZHG, No. 1.* 20-24 (in Russian).
- [4] Teterin M.P. 1967. Investigation of gas flow in the region of the shock drop Sealing on a cylinder, streamlined by a large supersonic flow Growth. In: *Izvestiya of the USSR Academy of Sciences, MZHG, No. 2.* 143-147 (in Russian).
- [5] Teterin M.P. 1967. Investigation of gas flow and heat transfer in the region Drop of the shock wave on the cylinder, streamlined by a large flow Supersonic speed. In: *Izvestiya of the USSR Academy of Sciences, MZHG, No. 3.* 92-97 (in Russian).
- [6] Avduevsky V.S., Medvedev K.I. 1968. The physical features of the flow in Three-dimensional separation zones. In: *Heat-mass transfer, vol. I.* Moscow, Energy. 140-147 (in Russian).
- [7] Borovoy V.Ya., Ryzhkov M.V. 1972. Heat transfer on a plate and a cone at Three-dimensional interaction of the boundary layer with a shock wave formed near the cylindrical obstacle. In: *Proceedings of TsAGI, No. 1374.* 166-185 (in Russian).
- [8] Borovoy V.Ya., Ryzhkova M.V. 1974. Heat transfer and gas flow during the interaction of the laminar boundary layer with a shock wave formed near the cylindrical obstacle. In: *Izvestiya of the USSR Academy of Sciences, MZHG, No. 1.* 78-87 (in Russian).
- [9] Hung F.T., El Segundo, Clauss J.M. 1980. Three-dimensional protuberance interference heating in high-speed flow. *AIAA Paper No. 80-0289.* 10.
- [10] Borovoy V.Ya., RyzhkovA M.V. 1977. Approximate calculation of the coefficients Heat transfer on a plate and a cone in the zone of interaction of the boundary layer with a shock wave formed near the cylindrical obstacle. In: *Proceedings of TsAGI, No. 1881.* 135-141 (in Russian).
- [11] Borovoy V.Ya., Pleshakova L.A., Ryzhkova M.V. 1982. Some features of heat exchange on the surface of a body near a cylindrical obstacle and a transverse jet. In: *Izvestiya of the USSR Academy of Sciences, MZHG, No. 3* (in Russian).
- [12] Mosharov V.E., Radchenko V.N. 2007. Measurement of heat flux fields in short-time pipes using luminescent temperature converters. In: *Uchenye Zapiski TsAGI, Vol. XXXVIII, No. 1-2.* 94-101 (in Russian).
- [13] Mosharov V.E., Radchenko V.N. 2010. A new method of visualizing currents on the surface of aerodynamic models. In: *Sensors and systems. No. 5.* 48 – 53 (in Russian).
- [14] Borovoy V.Ya. 1983. Gas flow and heat transfer in the zones of interaction of shock waves with a boundary layer. Moscow, Mashinostroenie. 141 (in Russian).